Supporting Information

Drury et al. 10.1073/pnas.1101133108

SI Materials and Methods

Bioluminescence Imaging. In accordance with protocols approved by the Medical College of Wisconsin Institutional Animal Care and Use Committee, highly metastatic HCT-Luc cells (2×10^6) were suspended in 50 μL sterile phosphate-buffered saline (PBS) and implanted to the subserosal layer of the cecum in 8-week-old male SCID mice (cr-*Prdkc*^{scid}, Charles River) following a midline laparotomy. Minimally metastatic HCT-luc-CXCL12 cells (2×10^6) were used as a control (1). Tumors were imaged 5 min after intraperitoneal (i.p.) injection of 200 μL [15 mg/mL] of D-luciferin (Xenogen Corporation). Mice were imaged immediately after implantation and then weekly using the Lumina IVIS-100 In Vivo Imaging System (Xenogen Corporation). CXCL12 treatments were administered biweekly in an i.p. injection of 200 μL beginning at 1-week postimplantation, and vehicle alone was used as a control. Mice were imaged for 1 min with medium binning and an f-stop of 1. Regions of interest were created and measured as area flux, defined by radiance (photons per seconds per square centimeter per steradian) according to the manufacturer's calibration (Xenogen Corporation). At end point, mice were euthanized and the intestinal tract from stomach through the colon and liver were extracted for ex vivo bioluminescence imaging.

Wound Migration Assays. HT29 cells were grown to confluence in serum-containing medium on 6-well plates (Corning Inc.). Cells were serum-starved 24 h and wounded using a bench top vacuum aspirator as we have previously defined (2, 3). Wounded epithelial monolayers were stimulated daily with CXCL12 variants for three days. Photomicrographs of circular wounds were taken using the 4× objective after wounding and 3 d postwounding. Migration was quantified using Metamorph (Molecular Devices) software to measure wound area at day 0 and day 3 time points. Eight wounds per treatment in each experiment were measured from three individual experiments.

Filamentous-Actin (F-Actin) Quantification. HCT116 cells (1×10^5) were plated for 24 h in serum-containing medium then serum-starved overnight. Cells were stimulated with either lysophosphotidic acid (LPA) or CXCL12 variants for 30 min, washed, and fixed in 4% (wt/vol) paraformaldehyde for 10 min. For siRNA based experiments, cells were serum-starved two days after transfection and stimulated the following morning. In separate experiments, cells were pretreated 30 min with pertussis toxin (800 ng/mL) prior to stimulation to assess Gαi-protein signaling or F-actin formation. Cells were then stained with Alexafluor-488 phalloidin in PBS with 0.3% (vol/vol) Triton X-100 for 20 min to visualize F-actin as previously described (2, 4). Mean fluorescence intensity per cell was obtained at 600× magnification and was quantified by tracing individual cells using Metamorph software. Thirty single cells were randomly selected and examined per treatment in three independent experiments.

Radioligand Binding Assays. HEK293E cells were transiently transfected as previously described (5) with 1 μg/well of CXCR4 or CXCR7 cDNA or empty vector. Twenty-four hours after transfection the medium was removed, the cells were incubated 5 min with 10 μM phenylarsine oxide (Sigma) to prevent endocytosis, followed by washing twice with PBS. Cells were then resuspended in binding buffer [50 mM HEPES, pH 7.4, 5 mM $MgCl_2$, 1 mM $CaCl_2$, and 0.2% (wt/vol) BSA] and seeded in 96-well plates in the presence of increasing concentrations of unlabeled competitor ligand. The competition studies were carried out at 37 °C for 30 min using 60 pM ^{125}I-CXCL12 (Perkin-Elmer Life and Analytical Sciences) as a tracer. A combi-cell harvester was used to wash the excess tracer and capture samples on glass-fiber filter paper (Molecular Devices). Binding was measured using a gamma-counter (Perkin-Elmer Life and Analytical Sciences). Experiments were carried out in duplicate.

In a complementary approach, commercial membrane preparations of cells stably expressing CXCR4 or CXCR7 were used (Millipore). Five micrograms of protein per point was incubated for 90 min on ice in binding buffer with 0.03 nM of ^{125}I-CXCL12 as a tracer and increasing concentrations of competitor in a final 40 μL volume. Bound radioactivity was separated from free ligand by filtration, and receptor-bound radioactivity was quantified by gamma-radiation counting. Isolated membrane binding experiments were carried out in duplicate.

Calcium Flux Assay. Intracellular calcium mobilization was measured as described previously (3, 6). Briefly, HCT116 cells were plated in 96-well white-walled plates (BD Biosciences Discovery Labware) and grown to 90% confluence. Cells were serum-starved overnight and loaded with cell permeant Fluo-4 AM (Invitrogen) diluted in calcium-free HBSS supplemented with 20 mM HEPES buffer and 2.5 mM probenecid provided by the manufacturer. For inhibition experiments, cells were treated with a CXCR4 specific antagonist, AMD3100 (5 μg/mL) or neutralizing antibody, 12G5 (10 μg/mL) for 30 min prior to chemokine addition. CXCL12 variants were diluted in calcium-free HBSS/HEPES buffer and added to each well for a 10 nM final concentration. Intracellular calcium flux was measured by fluorescence spectroscopy every 1.5 s for a total of 180 s (Victor3 Wallac, Perkin-Elmer Life and Analytical Sciences). Background fluorescence was measured 30 s prior to addition of ligand. Values were subsequently normalized to the average baseline fluorescence. Experiments were completed in 2–3 replicates on three separate days.

Bioluminescence Resonance Energy Transfer (BRET) Measurements. β-arrestin-2 recruitment was measured using an intermolecular BRET assay performed as described previously (7, 8). HEK293E cells were cotransfected with 1 mg of CXCR4-eYFP construct with 0.05 mg of β-arrestin-2-RLuc (a gift from Michel Bouvier, University of Montreal, Montreal, QC, Canada). For [acceptor]/[donor] titrations 0.05 mg of β-arrestin-2-RLuc were cotransfected with increasing amounts of the CXCR4-eYFP construct. All transfections were completed to 2 mg per well with empty vector. Following overnight culture, transiently transfected cells were seeded in 96-well, white, clear-bottom microplates (ViewPlate, Perkin-Elmer Life and Analytical Sciences), coated with poly-D-lysine, and left in culture for 24 h. Cells were washed once with PBS, and the RLuc substrate coelenterazine-H (NanoLight Technology) was added at a final concentration of 5 mM to BRET buffer [PBS, 0.5 mM $MgCl_2$, 0.1% (wt/vol) glucose]. β-arrestin recruitment was measured 30 min after ligand addition. The values were corrected to BRETnet by subtracting the background BRET signal obtained in cells transfected with RLuc construct alone.

For Epac/cAMP measurements, HEK293E cells were cotransfected with 1 μg of CXCR4 and 0.04 μg of an intramolecular Epac BRET^2 sensor. This sensor, GFP10-Epac-RLuc3, was a kind gift of Michel Bouvier (University of Montreal, Montreal, QC, Canada). Inhibition of forskolin-induced cAMP production

was measured as previously detailed (9). Ten minutes after addition of the BRET2 substrate (coelenterazine 400A; Biotium), the cells were stimulated with the indicated agonist in the presence of 20 μM forskolin, and BRET measurements were performed after additional 5 min incubation. BRET readings were collected using a Mithras LB940 plate reader (Berthold Technologies) and MicroWin2000 software. BRET measurement between Rluc and YFP was obtained by sequential integration of the signals detected in the 365- to 435-nm (RLuc3) and 505- to 525-nm (GFP10) windows. The BRET signal was calculated as the ratio of light emitted by acceptor (GFP10) over the light emitted by donor (Rluc3).

Immunoblot Analysis. Phosphorylation of ERK1/2 was assessed using specific antibodies as defined previously (1). Briefly, unstimulated and CXCL12 variant treated HT29 cells were solublized in modified RIPA buffer [50 mM Tris-HCl, pH 7.4, 150 mM NaCl, 0.25% (vol/vol) sodium deoxycholate, 1.0% (vol/vol) NP-40, 0.1% (vol/vol) SDS and 1 mM EDTA] supplemented with Protease Inhibitor Cocktail Set III (EMD Biosciences) and 10 mM sodium orthovanadate, 40 mM β-glycerolphosphate, and 20 mM sodium fluoride phosphatase inhibitors. Lysates were centrifuged at $10{,}000 \times g$ for 15 min at 4 °C. Protein concentration was determined using the Bradford protein assay (BCA kit, Pierce Biotechnology), and 10 μg of protein was size-separated using reducing SDS-PAGE. Proteins were electrophoretically transferred to PVDF membranes (Immobilon-P, Millipore), and levels of phosphorylated or total ERK1/2 were defined using specific antibodies as defined by the manufacturer (Cell Signaling Technology).

NMR Analysis. [U-^{15}N]-$CXCR4_{1–38}$ and [U-^{15}N]-CXCL12-variants were expressed and purified as previously described (10–12). NMR experiments were performed on a Bruker 600 DRX 600 equipped with $^{1}H/^{15}N/^{13}C$ TXI Cryoprobe at 25 °C. Titration of 250 μM [U-^{15}N]-$CXCR4_{1–38}$ with increasing unlabeled-$CXCL12_{WT}$ concentrations was measured by ^{15}N-^{1}H heteronuclear single-quantum coherence spectroscopy; sample conditions were 25 mM deuterated-MES buffer (pH 5.5), 10% (vol/vol) D_2O, and 0.02% (vol/vol) NaN_3. $CXCR4_{1–38}$ resonances were assigned by visual inspection based on previously published spectra (11). ^{15}N-^{1}H heteronuclear nuclear Overhauser effect experiments (10) were conducted on 250 μM [U-^{15}N]-$CXCR4_{1–38}$ in the above conditions alone, or in the presence of 500 μM $CXCL12_{H25R}$ or $CXCL12_2$.

Propidium Iodide Staining. HT29 or HCT116 (2×10^6) cells were plated in 6-well dishes, serum-starved overnight, and then stimulated with indicated CXCL12 variants for 24 h. Serum served as a positive control. Cells were lifted, fixed, and stained as previously described (13). The percentages of cells in G1 and G2/S were used to define cell cycling rates after treatment. Gating of sub-G1 indicated DNA degradation and cell death. Quantification of DNA content was conducted using a LSRII flow cytometer (BD Biosciences) and analyzed using FlowJo software.

Caspase 3/7 Activity Assay. HT29 or HCT116 (2×10^6) cells were plated in 6-well dishes, serum-starved overnight, and then stimulated with indicated CXCL12 variants for 24 h. Cells were collected, mixed at a 1:1 volumetric ratio with glo reagent, and incubated at room temperature for 30 min in the dark. Caspase-3/7 enzymatic activity was measured using specific caspase glo reagents (Promega) as luminescence units on the spectrophotometer (Victor3 Wallac). Gliotoxin [8 μg/mL], a known inducer of apoptosis, and zVAD [10 μg/mL] (EMD Chemicals), a pan-caspase inhibitor, served as positive and negative controls, respectively.

Silver Staining. Samples were size-separated on a 15% (vol/vol) polyacrylamide native gel at 180 V to separate dimeric and monomeric CXCL12 species. Separating gels were soaked twice in 50% (vol/vol) methanol washes for 15 min on a room-temperature shaker. Cells were further washed 20 min in 5% (vol/vol) methanol, 10 μM DTT, and then 0.1% (wt/vol) silver nitrate solution. Gels were washed briefly in water and then placed in developer solution containing 6% (wt/vol) sodium carbonate and 0.01% (vol/vol) formalin until bands intensified. The developer solution was stopped by addition of a 5% (wt/vol) citric acid solution.

β-Arrestin Knockdown. Previously reported small interfering RNAs (siRNAs) (14, 15) were chemically synthesized from Dharmacon. The siRNA sequences are β-arrestin-1, 5′-AAAGCCUUCUGCGCGGAGAAU-3′; β-arrestin-2, 5′-AAGGACCGCAAAGUGUUUGUG-3′; and β-arrestin-1/-2, 5′-ACCUGCGCCUUCCGCUAUG-3′. A nonsilencing RNA sequence was used as control, 5′-AAUUCUCCGAACGUGUCACGU-3′. For knockdown experiments, HCT116 cells were grown on coverslips in 6-well dishes. Twenty micrograms of siRNA was transfected into cells using lipofectamine 2000 reagent (Invitrogen). CXCL12 mediated F-actin formation was assayed as described above 48 h posttransfection.

RT-PCR. Total RNA was isolated from cultured cells using the QuaShredder and RNAeasy (Qiagen) according to manufacturer's protocols. RNA was DNase-treated (Ambion), and 2 μg of total RNA was converted to cDNA via reverse transcription using random priming in a 40 μL volume. GAPDH was amplified using previously described PCR primers and conditions (13). β-arrestin-1 and β-arrestin-2 were amplified using 28 cycles of 30-s denaturation at 95 °C, 30-s annealing at 60 °C, and 30-s extension at 72 °C. Primer sequences for β-arrestin-1 were 5′-CTGACCCCCTTCCTAGCCAATAA C-3′ and 5′-GGAAGAACAAAGGGGAAAAG AAAC-3′; β-arrestin-2 were 5′-CAGTGTGACGGAGCATGGAAGATT-3′ and 5′-CCCCAGCCCACAGCCG AGACCAC-3′. PCR products were size-separated using 1% (wt/vol) Tris/Borate/EDTA agarose gels and visualized following ethidium bromide staining.

Statistical Analyses. Differences in survival were analyzed using a Mantel–Cox test. Differences in bioluminescence between treatment groups was analyzed using a one-way ANOVA followed by Tukey's posttest (GraphPad Software Inc.). In vitro migration data were compared using an unpaired Student's t test. BRET data were the mean of independent experiments that were performed in triplicate and analyzed using a one-way ANOVA with Dunnett posttest. Curve-fitting by nonlinear regression and statistical analysis was conducted using Prism 4 software. Statistical significance of the differences between more than two groups was calculated by one-way ANOVA, followed by Tukey's posttest. Statistical significance was defined as $P \leq 0.05$.

1. Wendt MK, Drury LJ, Vongsa RA, Dwinell MB (2008) Constitutive CXCL12 expression induces anoikis in colorectal carcinoma cells. *Gastroenterology* 135:508–517.
2. Moyer RA, Wendt MK, Johanesen PA, Turner JR, Dwinell MB (2007) Rho activation regulates CXCL12 chemokine stimulated actin rearrangement and restitution in model intestinal epithelia. *Lab Invest* 87:807–817.
3. Agle KA, Vongsa RA, Dwinell MB (2010) Calcium mobilization triggered by the chemokine CXCL12 regulates migration in wounded intestinal epithelial monolayers. *J Biol Chem* 285:16066–16075.
4. Vongsa RA, Zimmerman NP, Dwinell MB (2009) CCR6 regulation of the actin cytoskeleton orchestrates human beta defensin-2- and CCL20-mediated restitution of colonic epithelial cells. *J Biol Chem* 284:10034–10045.
5. Kalatskaya I, Berchiche YA, Gravel S, Limberg BJ, Rosenbaum JS, Heveker N (2009) AMD3100 is a CXCR7 ligand with allosteric agonist properties. *Mol Pharmacol* 75:1240–1247.
6. Wendt MK, Cooper AN, Dwinell MB (2008) Epigenetic silencing of CXCL12 increases the metastatic potential of mammary carcinoma cells. *Oncogene* 27:1461–1471.

7. Gravel S, et al. (2010) The peptidomimetic CXCR4 antagonist TC14012 recruits {beta}-arrestin to CXCR7 roles of receptor domains. *J Biol Chem* 285:37939–37943.
8. Hamdan FF, Percherancier Y, Breton B, Bouvier M (2006) Monitoring protein-protein interactions in living cells by bioluminescence resonance energy transfer (BRET). *Curr Protoc Neurosci* Chapter 5:Unit 5.23.
9. Leduc M, et al. (2009) Functional selectivity of natural and synthetic prostaglandin EP4 receptor ligands. *J Pharmacol Exp Ther* 331:297–307.
10. Veldkamp CT, Peterson FC, Pelzek AJ, Volkman BF (2005) The monomer-dimer equilibrium of stromal cell-derived factor-1 (CXCL 12) is altered by pH, phosphate, sulfate, and heparin. *Protein Sci* 14:1071–1081.
11. Veldkamp CT, Seibert C, Peterson FC, Sakmar TP, Volkman BF (2006) Recognition of a CXCR4 sulfotyrosine by the chemokine stromal cell-derived factor-1alpha (SDF-1alpha/CXCL12). *J Mol Biol* 359:1400–1409.
12. Veldkamp CT, et al. (2008) Structural basis of CXCR4 sulfotyrosine recognition by the chemokine SDF-1/CXCL12. *Sci Signal* 1:ra4.
13. Drury LJ, Wendt MK, Dwinell, MB (2010) CXCL12 chemokine expression and secretion regulates colorectal carcinoma cell anoikis through Bim-mediated intrinsic apoptosis. *PLoS One* 5:e12895.
14. Ahn S, Wei H, Garrison TR, Lefkowitz RJ (2004) Reciprocal regulation of angiotensin receptor-activated extracellular signal-regulated kinases by beta-arrestins 1 and 2. *J Biol Chem* 279:7807–7811.
15. Gesty-Palmer D, et al. (2006) Distinct beta-arrestin- and G protein-dependent pathways for parathyroid hormone receptor-stimulated ERK1/2 activation. *J Biol Chem* 281:10856–10864.

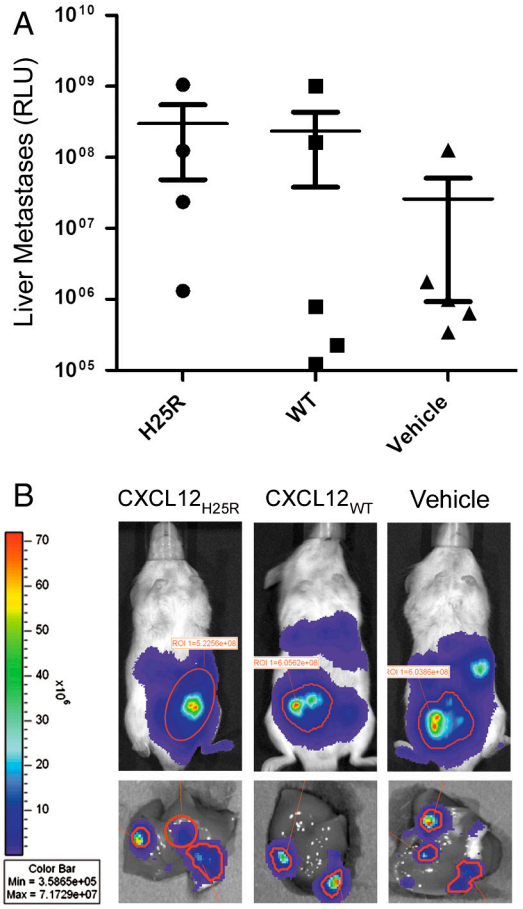

Fig. S1. Hepatic metastases in monomer (H25R) and wild-type (WT) CXCL12-treated mice. Mice were implanted with HCT116 luciferase expressing cells (2×10^6) and treated biweekly with 0.5 μM doses of $CXCL12_{H25R}$ or $CXCL12_{WT}$ 1-week postimplantation for 4 weeks. Vehicle (NaCl) served as control. (*A*) Data shown are liver metastases after 5 weeks of tumor growth. No statistical differences were seen between treatment cohorts analyzed using a one-way ANOVA analyzed followed by Tukey's posttest. (*B*) Shown are representative whole body (*Upper*) and ex vivo liver images after 5 weeks.

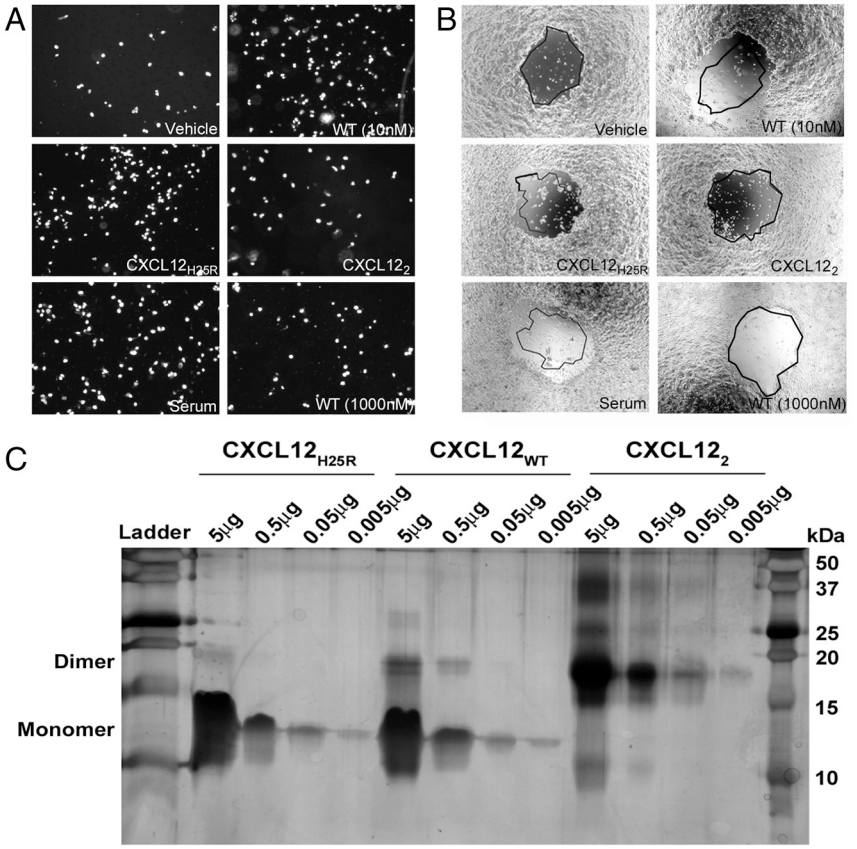

Fig. S2. Carcinoma cell migration is differentially regulated by monomeric and dimeric oligomers of CXCL12. (*A*) Chemotactic migration of HCT116 carcinoma cells is regulated by the chemokine monomer–dimer equilibrium. HCT116 chemotactic migration was induced after treatment with 10 nM monomer ($CXCL12_{H25R}$) and wild-type ($CXCL12_{WT}$). Dimeric ($CXCL12_2$) and supraphysiologic 1,000 nM concentrations of $CXCL12_{WT}$ weakly stimulated chemotactic migration. Vehicle and serum served as controls for baseline and positive cellular migration, respectively. (*B*) Oligomeric chemokines regulate epithelial sheet migration of HT29 carcinoma cells. $CXCL12_2$ (10 nM) or $CXCL12_{WT}$ (1,000 nM) were unable to induce cellular migration compared to 10 nM doses of $CXCL12_{H25R}$ or $CXCL12_{WT}$. Images shown are wounds at day 0 with the black outline indicating wound sizes 3 d postwounding. Data in *A* and *B* are representative of three separate experiments quantified and shown in Fig. 2 *A* and *B*. (*C*) Native PAGE analyses of wild-type ($CXCL12_{WT}$) chemokine confirms the presence of proteins with similar molecular weight as preferential-monomer ($CXCL12_{H25R}$) and locked-dimer ($CXCL12_2$). As expected from our prior reports, formation of dimeric protein is enhanced at increasing concentrations of wild-type protein. Higher molecular weight structures of the RP-HPLC purified protein were also apparent, consistent with the formation of larger oligomeric units. Data are representative of five separate analyses.

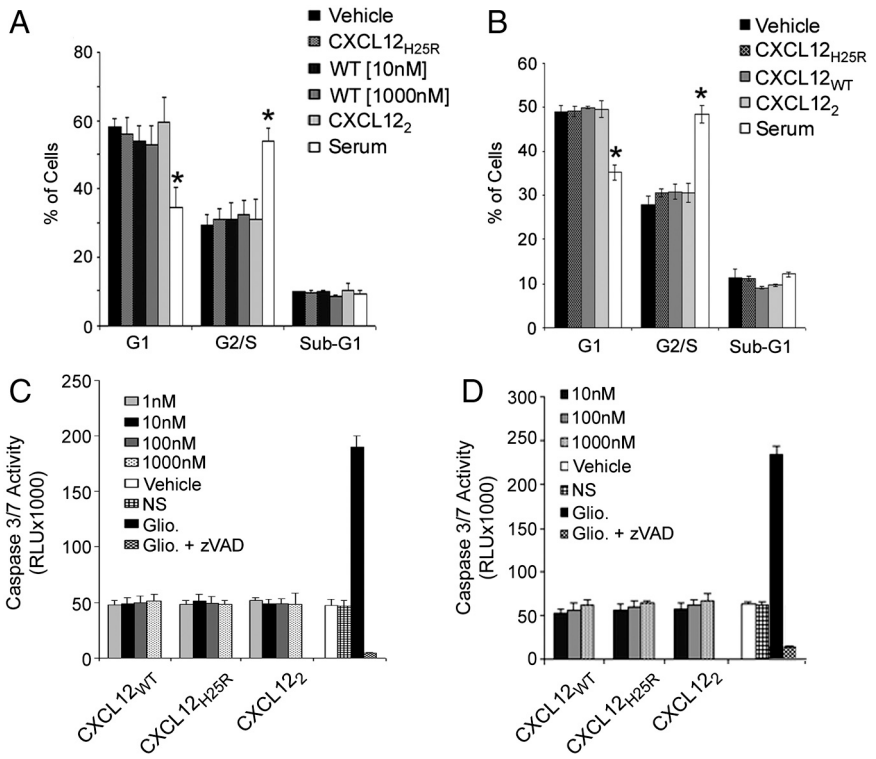

Fig. S3. Cell cycle progression and programmed cell death are unaffected by CXCL12 treatment. HCT116 (*A*) and HT29 (*B*) were serum-starved 24 h and then treated with 10 nM of either wild-type ($CXCL12_{WT}$), preferential-monomer ($CXCL12_{H25R}$), or locked-dimer ($CXCL12_2$) for 24 h. DNA content was analyzed using propidium iodide staining and gating for G2/S (cell cycle progression) and sub-G1 (cell death) populations following flow cytometry. Serum was used as a positive control for cellular proliferation. Values are mean ± SD of three independent experiments completed in duplicate. Asterisk indicates statistically significant from vehicle control ($P \leq 0.05$). HCT116 (*C*) and HT29 (*D*) cells were treated similarly as above with different concentrations of chemokine, and caspase-3/7 activity was quantified after 24 h using a luminescence-based assay. Gliotoxin, a known inducer of apoptosis, and zVAD, a pan-caspase inhibitor, served as controls. Data are representative of three independent experiments completed in duplicate. Values are mean ± SD. Asterisk indicates statistically significant from vehicle (NaCl) treated controls ($P \leq 0.05$).

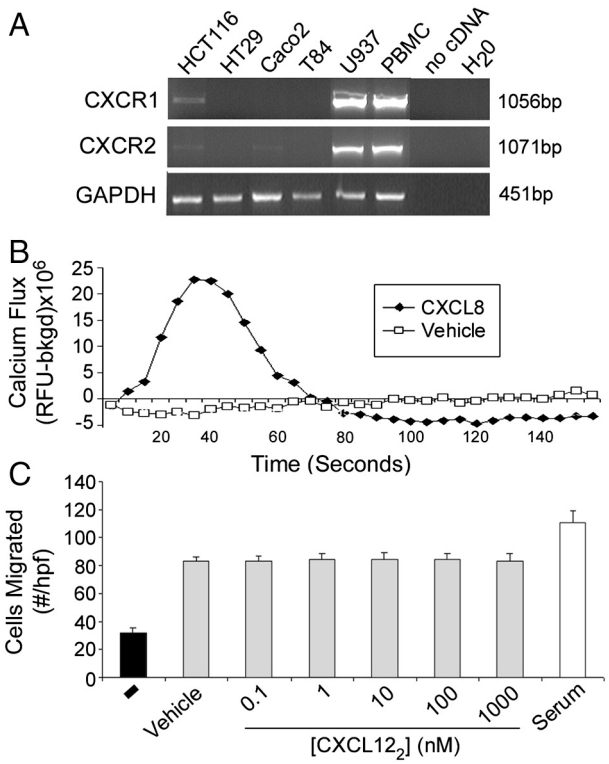

Fig. S4. CXCL12 locked-dimer does not competitively inhibit CXCL8-mediated chemotaxis. (*A*) RT-PCR analyses verified the expression of the CXCL8 receptor CXCR1 by HCT116 cells. In agreement with our prior work, CXCR1 and CXCR2 were minimally, if at all, expressed by HT29, Caco2, or T84 epithelial cells. Human U937 histiocytic leukemic cell line and peripheral blood monocytes were used as positive controls. (*B*) CXCL8 [100 nM] induced mobilization of intracellular calcium consistent with expression of functional CXCR1 by HCT116 cells. *C*) CXCL8 [100 nM] stimulated chemotactic migration of HCT116 cells, while increasing doses of the locked-dimer ($CXCL12_2$) were unable to inhibit CXCL8-induced migration. Serum was used as a positive control for transwell migration. Data in *A* and *B* are representative of three separate analyses. Values in *C* are mean ± SD.

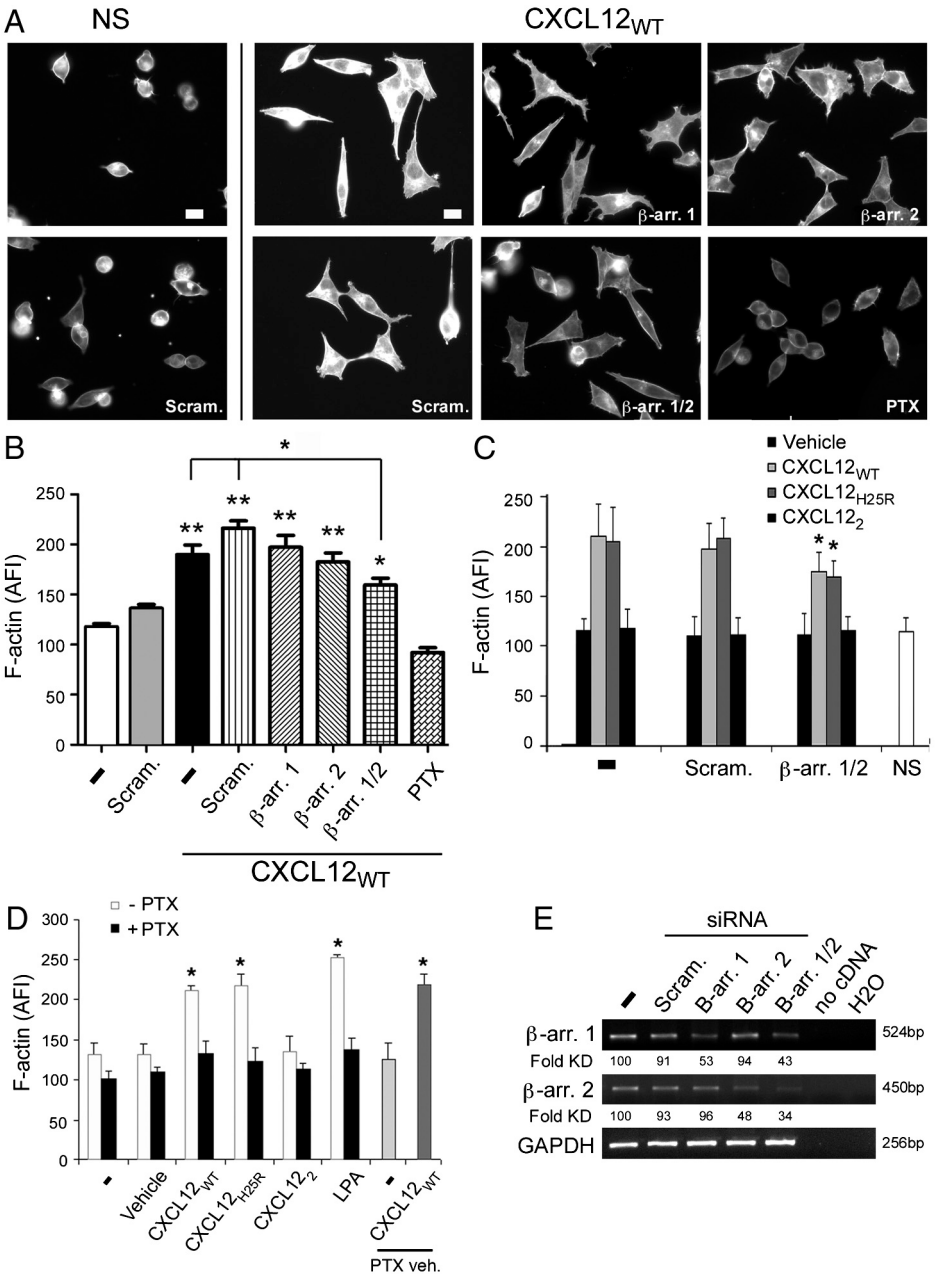

Fig. S5. CXCL12-induced F-actin formation. (*A*) HCT116 cells were transfected with siRNA 2 d prior to stimulation with 10 nM $CXCL12_{WT}$. To assess roles for Gαi-protein signaling in F-actin formation, HCT116 cells were pretreated 30 min with pertussis toxin (800 ng/mL) prior to stimulation. F-actin was visualized by phalloidin staining, and cells were imaged at 600× magnification. (*B*) F-actin was quantified using Metamorph software. Combinatorial knockdown of β-arrestin-1 and -2 (β-arr-1/2) significantly abrogated $CXCL12_{WT}$ stimulated accumulation of F-actin compared to untransduced (-) or scramble (Scram) cells. No statistical difference was observed between β-arrestin single or double knockdown cells. Addition of pertussis toxin (PTX) completely blocked CXCL12 mediated F-actin formation. Values are mean ± SD from three experiments and total 90 cells analyzed. Asterisk and double asterisk indicate statistical significance from unstimulated cells (-), $P \leq 0.05$ and $P \leq 0.01$ respectively. *C*) Knockdown of β-arrestin-1/-2 blocked $CXCL12_{WT}$ and $CXCL12_{H25R}$ mediated F-actin formation. $CXCL12_2$ stimulation was unable to elicit increased F-actin. Values are mean ± SD from three experiments, and asterisk indicates statistical significance from matched untransfected (-) and scramble (Scram) siRNA cells. (*D*) PTX pretreatment inhibited F-actin formation induced by 10 nM $CXCL12_{WT}$, 10 nM $CXCL12_{H25R}$, or 2 μg/mL LPA. Values are mean ± SD from three experiments, and asterisk indicates statistical significance from untreated (NS) control. (*E*) RT-PCR indicated efficient depletion of β-arrestin 48 h posttransfection in HCT116 cells. Fold knockdown was determined by densitometry and compared to untransfected transcript levels. Relative β-arrestin levels were normalized to GAPDH.

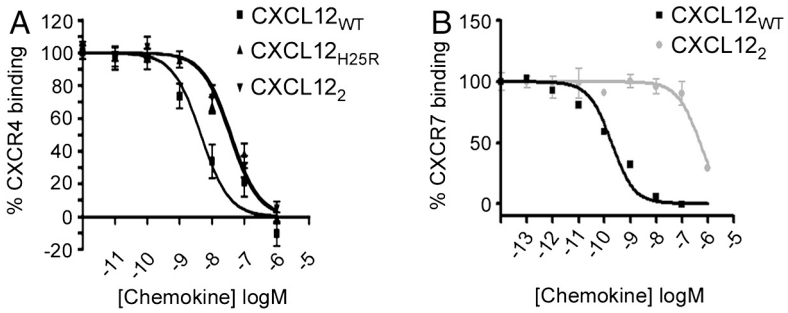

Fig. S6. Dimeric CXCL12 preferentially binds CXCR4. Radioligand binding assays using membrane preparations were completed as described in *SI Materials and Methods*. (*A*) $CXCL12_{H25R}$ and $CXCL12_2$ exhibit similar affinities for CXCR4 as determined by ^{125}I-CXCL12 displacement. K_d values for binding of $CXCL12_{WT}$, $CXCL12_{H25R}$, and the $CXCL12_2$ were calculated as 4.5, 40, and 35 nM, respectively, from their corresponding logEC50s of -8.34 ± 0.11, -7.40 ± 0.08, and -7.46 ± 0.08. (*B*) Radioligand displacement of CXCR7 showed weaker binding of $CXCL12_2$ (500 nM) compared to $CXCL12_{WT}$ (0.2 nM).

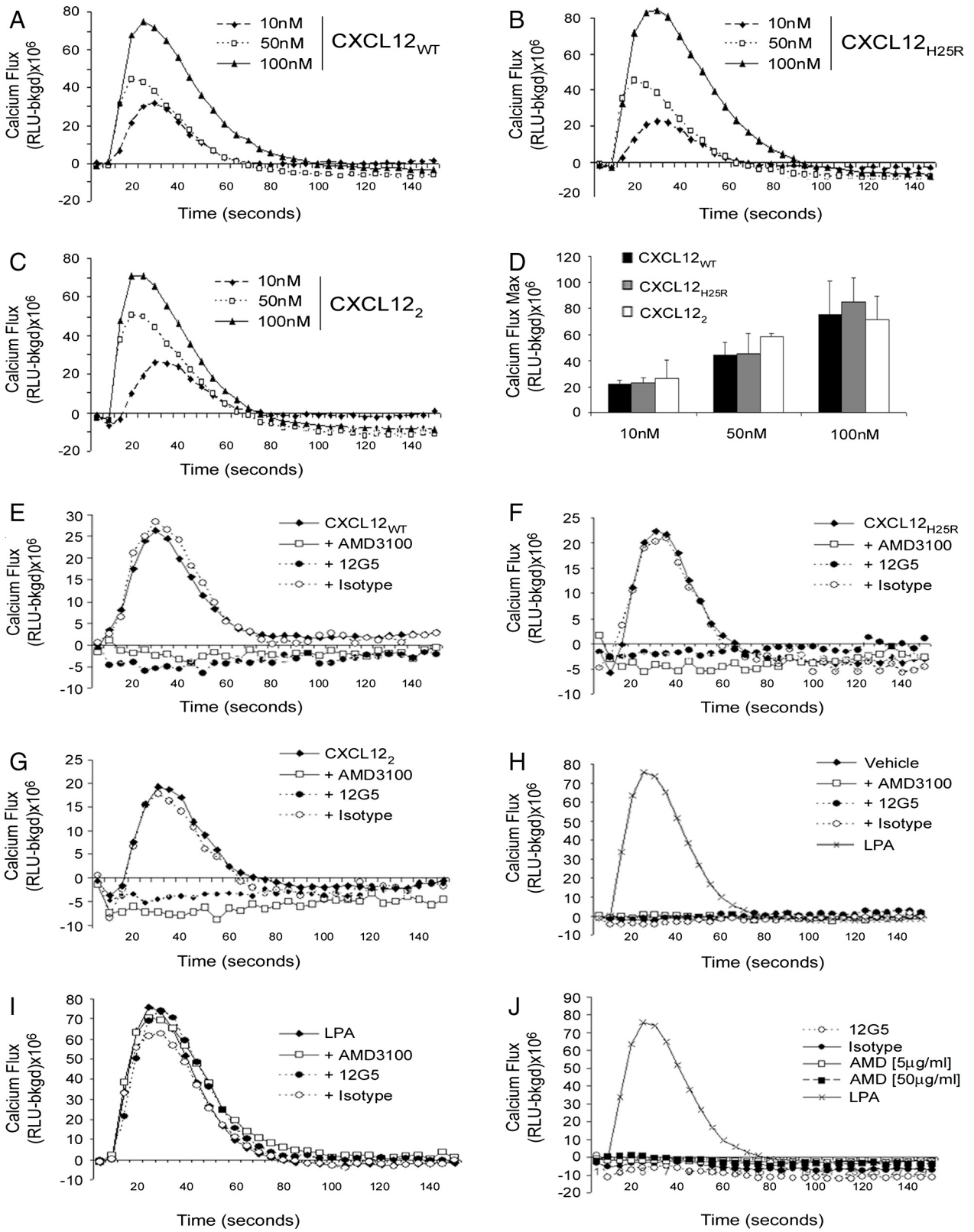

Fig. S7. CXCL12 variants similarly elicit calcium flux. (*A*) $CXCL12_{WT}$, (*B*) $CXCL12_{H25R}$, and (*C*) $CXCL12_2$ dose dependently increase mobilization of intracellular calcium. Data shown are representative of three separate analyses completed in duplicate. (*D*) Maximal calcium flux was alike between each CXCL12 variant at 10, 50, and 100 nM doses. Values are mean ± SD, $n = 3$. Wild-type ($CXCL12_{WT}$) (*E*), preferential-monomer ($CXCL12_{H25R}$) (*F*) and locked-dimer ($CXCL12_2$) (*G*) induced flux in intracellular calcium was blocked using the CXCR4 antagonist AMD3100 [5 μg/mL] or the neutralizing antibody (clone 12G5) at [10 μg/mL]. CXCR4 receptor inhibitor and neutralizing antibody alone did not stimulate calcium flux (*H* and *I*) and failed to block calcium mobilization elicited by LPA (1 μg/mL) (*J*). Data shown are representative of three separate analyses.

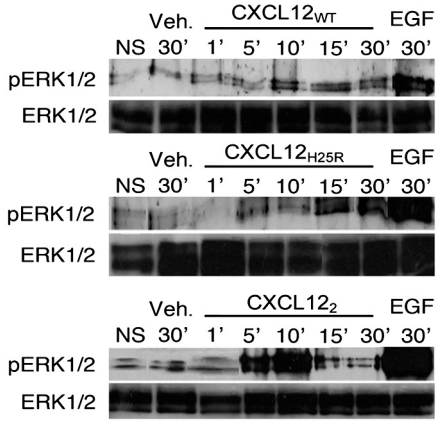

Fig. S8. CXCL12 variants differentially stimulate ERK1/2 phosphorylation. ERK1/2 phosphorylation was assessed over time in cells treated with 10 nM CXCL12 variants. Blots were stripped and reprobed with antibody specific for total ERK1/2 levels. Cells stimulated 30 min with epidermal growth factor (EGF) were a positive control. Unstimulated (NS) or treated with ligand vehicle (Veh.) served as negative controls. ERK1/2 phosphorylation was quantified as shown in Fig. 4 from independent immunoblot analyses. Data are representative of three separate experiments.